

Differential response of plant transpiration to uptake of rainwater-recharged soil water for dominant tree species in the semiarid Loess Plateau

Yakun Tang¹, Lina Wang¹, Yongqiang Yu¹, Dongxu Lu^{1,2}

5

¹ State Key Laboratory of Soil Erosion and Dryland Farming on the Loess Plateau, Institute of Soil and Water Conservation, Northwest A&F University, Yangling, 712100, China

² State Key Laboratory of Soil Erosion and Dryland Farming on the Loess Plateau, Institute of Soil and Water Conservation, Chinese Academy of Sciences, Ministry of Water Resources, Yangling, 712100,

10 China

Correspondence to: Yakun Tang (t453500@163.com)

Abstract Whether uptake of rainwater-recharged soil water (RRS) can increase plant transpiration in response to rainfall pulses requires investigation to evaluate the plant adaptability, especially in water limited regions where rainwater is the only replenishable soil water source. In this study, the water sources from RRS and three soil layers, predawn (Ψ_{pd}), midday (Ψ_m) and gradient ($\Psi_{pd}-\Psi_m$) of leaf water potential, and plant transpiration in response to rainfall pulses were analyzed for two dominant tree species, *Hippophae rhamnoides* subsp. *sinensis* and *Populus tomentosa*, in pure and mixed plantations during the growing period (June–September). In pure plantations, the relative response of daily normalized sap flow (SF_R) was significantly affected by RRS uptake proportion (RUP) and $\Psi_{pd}-\Psi_m$ for *H. rhamnoides*, and was significantly influenced by $\Psi_{pd}-\Psi_m$ for *P. tomentosa* ($P < 0.05$). Meanwhile, the large $\Psi_{pd}-\Psi_m$ was consistent with high SF_R for *H. rhamnoides*, and the small $\Psi_{pd}-\Psi_m$ was consistent with the low SF_R for *P. tomentosa*, in response to rainfall pulses. Therefore, *H. rhamnoides* and *P. tomentosa* exhibited sensitive and insensitive responses to rainfall pulses, respectively. Furthermore, mixed afforestation significantly enhanced RUP, SF_R , and reduced the water source proportion from the deep soil layer (100–200 cm) for both species ($P < 0.05$). The SF_R was

25

significantly influenced by RUP and $\Psi_{pd}-\Psi_m$ for both species in the mixed plantation. Lower Ψ_m and higher Ψ_{pd} were adopted by *H. rhamnoides* and *P. tomentosa* in mixed plantation, respectively, to
30 enlarge $\Psi_{pd}-\Psi_m$ and enhance RRS uptake. These results indicate that mixed afforestation enhanced the influence of RRS uptake to plant transpiration for these different rainfall pulse sensitive plants. This study provides insights into suitable plantation species selection and management considering the link between RRS uptake and plant transpiration in water limited regions.

35 **Keywords:** Leaf water potential; Loess Plateau; Plant transpiration; Rainwater-recharged soil water; Water stable isotope

1 Introduction

Rainwater-recharged soil water (RRS) uptake by plants and plant transpiration in response to rainfall
40 pulses drive the survival of plant species and ecosystem ecohydrological processes, especially in arid and semiarid regions where rainwater is the only replenishable soil water source (Berkelhammer et al., 2020; Gebauer and Ehleringer, 2000; West et al., 2012). Generally, RRS uptake after a rainfall pulse refers to the root uptake of soil water that was recharged by recent rainwater, and can be quantified through water stable isotopes (Cheng et al., 2006; Meier et al., 2018). The variability and intermittency
45 of rainfall, which plays an important role in plant water uptake and transpiration (Swaffer et al., 2014; Wang et al., 2020a), have been predicted to increase in water limited regions (Mendham et al., 2011). Clarifying the influence of RRS uptake on plant transpiration after rainfall pulses is essential to understand the process of plant species adaptation in water limited regions (Meier et al., 2018; Tfwala et al., 2019).

50 The RRS uptake by plant is expected to increase plant transpiration after a rainfall pulse (Cheng et al., 2006; Liu et al., 2019). However, the uptake of RRS may also be mainly used to reduce the water uptake from deep soil layers or decrease the risk of cavitation in stems for some plant species (Plaut et al., 2013; Tfwala et al., 2019). The controversial rainfall pulse response between RRS uptake and plant transpiration may be mainly attributed to an inconsistent influence of plant leaf physiological

55 characteristics (West et al., 2007), root morphology adjustment (Wang et al., 2020a), or environmental conditions (Tfwala et al., 2019) on these two water processes. Generally, plant transpiration is observed to increase after rainfall pulses for plants with shallow (Liu et al., 2019) or dimorphic root systems (Swaffer et al., 2014); meanwhile, no increase or a decrease in plant transpiration is observed for plants with deep rooting systems (West et al., 2012). However, regardless of the root distribution, the plant
60 leaf water potential gradient (the difference between predawn (Ψ_{pd}) and midday (Ψ_m) leaf water potential) has been observed to regulate plant transpiration after rainfall pulses (Kumagai and Porporato, 2012; Liu et al., 2019). Thus, taking into consideration plant leaf physiological or root morphological parameters could help in understanding the mechanisms underlying the influence of RRS uptake on plant transpiration in response to rainfall pulses.

65 Uptake of contrasting water sources between coexisting species usually shows water source separation and can minimize water source competition (Munoz-Villers et al., 2020; Silvertown et al., 2015); however, overlapping water sources among plant species may lead to competition in arid and semiarid regions (Tang et al., 2019; Yang et al., 2020). Rainfall pulses have been observed to relieve or eliminate water competition among coexisting species and thus maintain or increase plant transpiration
70 in some water limited regions (Wang et al., 2020a; Tfwala et al., 2019). Meanwhile, plant species with strong RRS uptake ability generally exhibit more competitiveness than coexisting weak RRS uptake ability species (Stahl et al., 2013; West et al., 2012). However, Liu et al. (2019) attribute opposite RRS uptake ability to the stable coexistence of species in mixed plantations in semiarid regions, where the rainfall events are variable and less RRS taken up by one of the coexisting plant species. In addition,
75 coexisting species may also cope with or minimize water resource competition through plant leaf water potential or root distribution adjustment (Chen et al., 2015; Silvertown et al., 2015). It is still unclear whether these adjustments could influence the RRS uptake and plant transpiration for coexisting species in water limited regions.

The “Grain for Green project” has increased vegetation coverage by 25% in the Loess Plateau
80 through afforestation activities since the 1990s, to deal with vegetation degradation and water and soil loss (Tang et al., 2019; Wu et al., 2021). *Hippophae rhamnoides* subsp. *sinensis* and *Populus tomentosa*

are typical deciduous broadleaved tree species, with similar leaf expansion (April) and falling (November) periods, and occupy nearly 30% of the plantation area in this region (Liu et al., 2017; Tang et al., 2019). Our previous study indicated that *H. rhamnoides* generally took up soil water from 0–40
85 cm or > 100 cm soil depths and adopted large leaf water potential variation to cope with varied soil water conditions in this region (Tang et al., 2019). Meanwhile, *P. tomentosa* generally took up soil water from > 100 cm soil depth throughout the growing season in varied soil water conditions (Xi et al., 2013). In addition, mixed plantations of these two species were widely promoted by local government due to the higher soil and water conservation capacity than pure plantations in the original afforestation
90 stage (Tang et al., 2019; Wang et al., 2020a). Tang et al. (2019) also suggested that mixed afforestation with *Ulmus pumila*, a deciduous broadleaved tree species with similar leaf growth phenology to *H. rhamnoides*, increased the water source from 0–40 cm soil depth and enlarged the leaf water potential variation for *H. rhamnoides* compared with these values for this species in pure plantation. Furthermore, rainfall events have obvious seasonal variability and the rainfall amount is generally lower than the
95 reference evapotranspiration (ET_0) during the plant growth period in this semiarid region (Zhang et al., 2017). The imbalance between rainwater input and plant water demand may weaken the sustainability of plantations with further plant growth (Jia et al., 2020; Wu et al., 2021). To understand the adaptation of plantation species in this study, the plant transpiration, water sources from RRS and different soil layers, and plant leaf water potential for *H. rhamnoides* and *P. tomentosa* in pure and mixed plantations
100 were analyzed. The specific objectives were as follow: (1) to investigate the influence of RRS uptake and leaf water potential on plant transpiration after rainfall events in pure plantation, and (2) to assess the mixed afforestation effect on these influences. Based on variations of plant water uptake from different soil layers and leaf water potential for these species in Xi et al. (2013) and Tang et al. (2019), we hypothesize that (1) the influence of RRS uptake and leaf water potential on plant transpiration may
105 differ for these species in pure plantations, and (2) these influences may differ for specific species in pure and mixed plantations.

2 Materials and methods

2.1 Study site

110 The study was conducted in the Ansai Ecological Station in the semiarid Loess Plateau (36.55 N, 109.16 E, 1221 m above sea level), Northern China (Fig. S1). The study area has a semiarid continental climate. The annual average (mean \pm SD) rainfall amount and air temperature are 454.8 ± 105.2 mm and 10.6 ± 0.4 °C (2000–2017), respectively, with higher monthly rainfall amount and air temperature generally occurring during June–September and lower values during the other months (Fig. S1).

115 Three adjacent plantations were chosen for the study: pure *H. rhamnoides* plantation, pure *P. tomentosa* plantation, and *H. rhamnoides*–*P. tomentosa* mixed plantation (Fig. S1), with corresponding plantation slope of 5.2, 4.5, and 5.5°. All plantations were planted on abandoned grassland in 2004, where *Bothriochloa ischaemum* was the dominant herbaceous species at that time. Three adjacent plots were selected (16 m \times 10 m) for each plantation type, and no soil and water conservation measure was
120 conducted in the plantations. In pure plantations, the original planted spacing for each individual plant was 2.0 m \times 2.0 m. In the mixed plantation, *P. tomentosa* was originally planted between the 4.0 m gaps in rows of *H. rhamnoides*, each individual plant was also spaced 2.0 m \times 2.0 m. Based on a survey performed in July 2018, in pure plantations, the average tree trunk diameter (at 1.2 m height above the ground) and height were 50.5 ± 3.6 mm and 4.11 ± 0.81 m for *H. rhamnoides*, respectively, and the
125 corresponding values were 52 ± 4.6 mm and 4.05 ± 0.63 m for *P. tomentosa*. Meanwhile, in mixed plantations, the average trunk diameter and tree height were 51.3 ± 2.9 mm and 4.49 ± 0.7 m for *H. rhamnoides*, respectively, and the corresponding values were 56.3 ± 3.8 mm and 4.23 ± 0.79 m for *P. tomentosa*. *B. ischaemum* and *Glycyrrhiza uralensis* were the dominant herbaceous species in *H. rhamnoides* and *P. tomentosa* pure plantations, respectively; meanwhile, *B. ischaemum* was dominant in
130 the mixed plantation. Based on an experiment conducted in July 2018 using the cutting ring (Wu et al., 2016) and constant water head (Reynolds et al., 2002) method, the soil bulk density, total porosity, and saturated hydraulic conductivity at 0–50 cm soil depth were similar in three plantations. The average soil bulk density was 1.34 ± 0.04 , 1.31 ± 0.05 , and 1.31 ± 0.05 g cm⁻³ for pure *H. rhamnoides*, pure *P. tomentosa*, and mixed plantations, respectively, and corresponding soil total porosity was 48.25 ± 0.52 ,
135 48.17 ± 0.48 , and $48.03 \pm 0.63\%$. The average soil saturated hydraulic conductivity was 0.51 ± 0.15 ,

0.54 ± 0.13, and 0.53 ± 0.11 mm min⁻¹ for pure *H. rhamnoides*, pure *P. tomentosa*, and mixed plantations, respectively. The soil is characterized as a silt loam soil according to United States Department of Agriculture soil taxonomy, with average sand (2–0.05 mm), silt (0.05–0.002 mm), and clay (<0.002 mm) compositions were 24.7 ± 1.6, 62.7 ± 0.8, and 12.6 ± 1.8%, respectively, for three
 140 plantation types at 0–50 cm soil depth. These compositions were determined using a Mastersize 2000 (Malvern Instruments Ltd., UK).

2.2 Environmental parameter measurements and ET₀ calculation

Net radiation (R_n, CNR4, Kipp & Zone Inc., Netherlands), atmospheric pressure (CS105, Vaisala Inc.,
 145 Finland), air temperature (T_a) and relative humidity (HMP45D, Vaisala Inc.), and wind velocity (W_s, A100R, Vector Inc., UK) were measured using a weather station nearly 500 m from the research plots. Soil heat flux (G) and rainfall amount were measured at 5 cm below ground using two HFT-3 plates (Campbell Scientific Inc., USA) and a TE525 rain gauge (Campbell Scientific Inc.), respectively. At each plot, soil water content (SW) was measured at 5, 20, 50, 100, 150, and 200 cm below ground
 150 (SW_{5cm}, SW_{20cm}, SW_{50cm}, SW_{100cm}, SW_{150cm}, and SW_{200cm}) by CS615 probes (Campbell Scientific Inc.). All these parameters were measured and stored at 30 min interval by a CR3000 datalogger (Campbell Scientific Inc.).

ET₀, considering both aerodynamic characteristics and energy balance, was used to indicate atmospheric evaporative demand (Allen et al., 1998):

$$155 \quad ET_0 = (0.408 \times s \times (R_n - G) + \gamma \times \frac{900}{T_a + 273} \times W_s \times VPD) / (s + \gamma \times (1 + 0.34 \times W_s)) \quad (1)$$

where γ , s , and VPD are the psychrometric constant (kPa K⁻¹), the slope between saturation vapor pressure and air temperature (kPa K⁻¹), and vapor pressure deficit (kPa), respectively. The units of R_n and G are W m⁻², and of W_s is m s⁻¹.

160 2.3 Sap flow observation

Three standard individuals, with approximately mean height and trunk diameter, for specific species

were chosen in each of the nine plots (Table S1). In each plot in the mixed plantation, three individuals of *H. rhamnoides* were chosen firstly, then a neighboring *P. tomentosa* individual was selected at approximately 2 m distance from each chosen *H. rhamnoides* individual. The sap flow was monitored by a pair of Granier-type thermal dissipation probes (TDPs) 10 mm in length and 2 mm in diameter in 36 selected individuals. During the plant growing season and ranging from 1 June (DOY 152) to 30 September (DOY 273) in 2018, the 30 s original and 30 min average sap flow values were monitored using a CR3000 data logger (Campbell Scientific Inc.). Waterproof silicone and aluminum foil were used to avoid the impact of the external environment on and physical damage to TDPs (Du et al., 2011). The standard sap flow density (F_d , ml m⁻² s⁻¹) was calculated as follows (Granier, 1987):

$$F_d = 119((\Delta t_{\max} - \Delta t) / \Delta t)^{1.231} \quad (2)$$

where Δt and Δt_{\max} are the temperature difference of heated and unheated probes at 30 min intervals and the maximum Δt in each day, respectively.

Steppe et al. (2010) suggested that F_d should have a species-specific calibration to validate Eq. (2). Meanwhile, the possibility of underestimating the F_d value with the Granier-type thermal dissipation method (Du et al., 2011) should be considered when the whole tree transpiration is calculated. However, with the lack of species-specific calibration for Eq. (2) in the present study, the daily normalized F_d for each replicate individual was calculated as the index of plant transpiration, through dividing F_d by the maximum value from DOY 152 to DOY 273. Thus, each monitored individual had a maximum daily normalized F_d of 1. In each plantation type, the average daily normalized F_d for specific species was calculated in each plot to determine the plant transpiration characteristics rather than the absolute transpiration amount (Du et al., 2011).

2.4 Rainwater, plant stem, soil water, and leaf sample collection and measurement

From April to October 2018, at the end of each rainfall event, 19 rainwater samples were collected immediately using a polyethylene rain gauge cylinder placed in the weather station, and stored at 4 °C. A funnel containing a ping-pang ball was connected at the top of rain gauge cylinder to avoid rainwater evaporation (Yang et al., 2015). To avoid the influence of sample collection on sap flow observation,

one standard individual for the specific species nearby each sap flow monitored individual was selected
190 for plant stem and soil water collection. In the mixed plantation, the distance was approximately 2 m
between the selected *H. rhamnoides* and *P. tomentosa* standard individuals in each plot for sample
collection. For plant stem and soil water collection, 5 rainfall events were selected: 3.4 mm (DOY 194),
7.9 mm (DOY 266), 15.4 mm (DOY 249), 24 mm (DOY 204), and 35.2 mm (DOY 155–156). These
rainfall events were selected with an interpulse period longer than 7 days to eliminate the potential
195 influence of the previous rainfall event. In addition, no runoff was generated during the selected rainfall
events in three plantations according to the simulated result from the HYDRUS-1D model (Appendix
A), which is based on the Richards' equation to describe soil water dynamics (Šimůnek et al., 2008). This
model has been widely used to simulate the runoff and soil water dynamics in the Loess Plateau (Yi and
Fan, 2016; Bai et al., 2020; Wang et al., 2020b).

200 At each of successive three days after every selected rainfall event, one suberized stem after
removing the bark was collected at midday (11:30–13:30) for each standard individual. Meanwhile,
approximately 0.5 m around the stem of each standard individual in the pure plantations and at the
middle between two species in the mixed plantation, one soil core at seven depths (0–10, 10–20, 20–30,
30–50, 50–100, 100–150, and 150–200 cm) was collected through soil drilling. The suberized stem and
205 collected soil samples were placed into glass bottles. These bottles were sealed with parafilm and stored
at $-15\text{ }^{\circ}\text{C}$. On the same day as plant stem and soil sample collections, one leaf was selected from each
sap flow monitored individual for leaf water potential measurement. The Ψ_{pd} and Ψ_{m} were measured by
a PMS1515D analyzer (PMS Instrument, Corvallis Inc., OR, USA) at predawn (4:30–5:30) and midday
(11:20–12:40), respectively.

210 All the plant stem, soil, and leaf samples collected on the first day after a rainfall pulse were used for
analysis, with the detailed given in section “2.6 Statistical analysis”. There were 180 stem and 945 soil
samples for water extraction, and 180 leaf samples for Ψ_{pd} and Ψ_{m} measurement, respectively.

A vacuum line (LI-2100, LICA Inc., China) was used to extract water from soil samples and plant
stems. The water isotopic values of rainwater, soil samples, and plant stems were determined using a
215 DLT-100 water isotope analyzer (LGR Inc., USA), with accuracy of ± 0.1 ($\delta^{18}\text{O}$) and ± 0.3 ‰ (δD).

The potential influence of organic matter on water isotopic values produced during water extraction from stems was eliminated using the method of Yang et al. (2015). The isotopic values (‰) were calculated as follows:

$$\delta^{18}\text{O}(\text{D}) = (R_{\text{sample}} - R_{\text{standard}}) / R_{\text{standard}} \times 1000\text{‰} \quad (3)$$

220 where R_{standard} and R_{sample} indicate the $^{18}\text{O}/^{16}\text{O}$ (D/H) molar ratios of water sample relative to the Vienna Standard Mean Ocean Water, respectively. The average water $\delta^{18}\text{O}$ and δD of plant stems for specific species and corresponding soil samples was calculated in each plot for further analysis.

2.5 Plant fine root investigation

225 In August 2018, 4 soil cores were dug around each selected standard individual for plant stem and soil water collection, through a soil drill with diameter 20 cm to investigate plant fine roots. The collected soil depths were 0–10, 10–20, 20–30, 30–50, 50–70, 70–100, 100–130, 130–150, 150–200 cm, with approximately 0.5 m around the stem of each species standard individual. The sum of root samples for 4 soil cores at each soil depth for each selected standard individual was used for fine root distribution
230 analysis, giving 324 fine root samples. WinRHIZO (Regent Instruments Inc., Quebec, Canada) was used to determine the fine root (diameter < 2 mm) surface area at each soil depth. The average fine root surface area for specific species at each soil depth was calculated in each plot for further analysis.

2.6 Statistical analysis

235 2.6.1 Plant transpiration and leaf water potential in response to rainfall pulse calculation

In the present study, the first day after rainfall was the maximum normalized F_d within 3 days for *H. rhamnoides* and *P. tomentosa* in both plantation types, except that the second day after 24 and 35.2 mm was the maximum normalized F_d for *P. tomentosa* in pure plantation. However, for *P. tomentosa* in pure plantation, there was no significant difference ($P > 0.05$) in diurnal sap flow between the first and
240 second day after each of these two rainfall events based on independent-sample *t*-test (Fig. S2). Therefore, the normalized F_d on the first day after each selected rainfall amount was used in Eq. (4) to calculate the relative response of daily normalized F_d (SF_R , %) to rainfall pulses:

$$SF_R = ((X_{after} - X_{before}) / X_{before}) \times 100\% \quad (4)$$

where X_{after} and X_{before} are the normalized F_d on the first day after and on the day before the rainfall event, respectively.

Meanwhile, none of Ψ_{pd} , Ψ_m nor $\Psi_{pd} - \Psi_m$ showed significant differences between the first and second day after each rainfall event ($P > 0.05$) for these two species in both plantation types (Table S2). On the first day after each rainfall event, the average Ψ_{pd} , Ψ_m , and $\Psi_{pd} - \Psi_m$ for specific plant species in each plot were used in the following analysis to illustrate the influence of leaf water potential on SF_R in response to rainfall pulses.

2.6.2 Calculation of RRS uptake proportion and water sources from different soil layers

The RRS uptake proportion (RUP, %) after a recent rainfall pulse for plant was calculated as the proportion of rainwater in plant stem as follows (Cheng et al., 2006):

$$\delta^{18}\text{O}(\text{D})_p = RUP \times \delta^{18}\text{O}(\text{D})_{\text{rain}} + (1 - RUP) \times \delta^{18}\text{O}(\text{D})_{\text{swb}} \quad (5)$$

$$RUP = (\delta^{18}\text{O}(\text{D})_p - \delta^{18}\text{O}(\text{D})_{\text{swb}}) / (\delta^{18}\text{O}(\text{D})_{\text{swa}} - \delta^{18}\text{O}(\text{D})_{\text{swb}}) \times 100\% \quad (6)$$

where $\delta^{18}\text{O}(\text{D})_{\text{rain}}$ and $\delta^{18}\text{O}(\text{D})_p$ are the isotopic values for rainwater and plant stem after rainfall, respectively; $\delta^{18}\text{O}(\text{D})_{\text{swb}}$ and $\delta^{18}\text{O}(\text{D})_{\text{swa}}$ are the isotopic values of soil water immediately before and after rainfall, respectively. The Eq. (6) is derived through the linear mixing model for water isotopic value in plant stem after rainfall in Eq. (5). The RUP was the average value calculated in Eq. (6) based on $\delta^{18}\text{O}$ and δD , respectively, for specific plant species in each plot.

Equations (5) and (6) are based on the assumption that little or no soil water is lost through evaporation. Thus, in this study, only the values of plant stem and soil water collected on the first day immediately after rainfall were used, and only the RUP on the first day after each rainfall event was calculated.

In this study, the $\delta^{18}\text{O}(\text{D})_{\text{swb}}$ could not be directly and accurately determined through soil water sample collection, due to unpredictable natural rainfall events. A linear mixed model can be used to calculate the $\delta^{18}\text{O}(\text{D})_{\text{swb}}$, based on the isotopic values for rainwater and soil water after rainfall, and soil

depth interval weighted SW before ($SW_b, m^3 m^{-3}$) and after ($SW_a, m^3 m^{-3}$) rainfall:

$$\delta^{18}O(D)_{swb} = SW_b/SW_a \times \delta^{18}O(D)_{swa} + (1 - SW_b/SW_a) \times \delta^{18}O(D)_{rain} \quad (7)$$

270 In addition to RUP, the water uptake proportions from different soil layers were calculated on the first day after a rainfall event using the MixSIR program, to complement the analysis of plant water source variations in response to rainfall pulses. The RUP method only calculated the proportion of recent rainwater in the plant stem and did not include soil water before the recent rainfall event (Gebauer and Ehleringer, 2000; Cheng et al., 2006). The water taken up from different soil layers by the plant is a
275 mixture of soil water before the recent rainfall event and the recent rainwater.

Firstly, the seven soil depths (0–10, 10–20, 20–30, 30–50, 50–100, 100–150, and 150–200 cm) were combined into three soil layers (shallow, middle, and deep) based on the variation of soil water $\delta^{18}O$ and δD and SW, to facilitate water source comparison (Wang et al., 2020a; Zhao et al., 2021). The shallow (0–30 cm) soil layer was vulnerable to rainfall, which exhibited high soil water $\delta^{18}O$ and δD
280 values and large water isotope and SW variations (Table S3, Fig. S3). The middle (30–100 cm) soil layer was less vulnerable to rainfall, with moderate soil water isotope values and water isotope and SW variations. The deep (100–200 cm) soil layer was relative stable, with lower soil water isotope values and smaller water isotope and SW variations compared with shallow and middle soil layers. In addition, based on one-way ANOVA followed by post hoc Tukey's test, significant difference ($P < 0.05$) was
285 observed in soil water $\delta^{18}O$ and δD among three soil layers in each plot. Then, the water uptake proportions from three soil layers were calculated using the MixSIR program (Moore and Semmens, 2008), with model input parameters being the average $\delta^{18}O$ and δD values in plant stem water and soil water at each soil layer in each plot. The SD for $\delta^{18}O$ and δD at each soil layer was also used to accommodate the uncertainties of these values. No fractionation was considered during water source
290 uptake by these plant roots because none of the plants exhibited xerophytic or halophytic characteristics. Ellsworth and Williams (2007) and Moore and Semmens (2008) suggested that a water stable isotope fractionation generally occurred during root uptake by xerophytic or halophytic plants.

2.6.3 Statistical analysis for plant transpiration, water sources, and leaf water potential in response to rainfall pulse

295 A repeated ANOVA (ANOVAR) was used to analyze the differences in plant transpiration, water
sources, and plant physiological parameters between these species in pure and mixed plantations,
respectively. This analysis was conducted with SF_R , RUP, relative water uptake proportions from three
soil depths, and $\Psi_{pd} - \Psi_m$ as response variables, and “species” and “rainfall” as between-subject and
within-subject factors, respectively. The same analysis was used to detect mixed afforestation effect on
300 response variables for each plant species, with “plantation type” and “rainfall” as between-subject and
within-subject factors, respectively. Furthermore, significant differences in fine root proportion for each
soil layer (shallow, middle, and deep) for specific species between pure and mixed plantations were
detected through independent-sample *t*-test. All of these analyses were calculated with SPSS 18 (IBM
Inc., New York, US), after data normal distribution and homogeneity of variance analysis were tested.

305

3 Results

3.1 Variation in environmental parameters and plant fine root vertical distribution

The rainfall amount during the study period (262.7 mm, DOY 152–273) was 15.56% lower than the
average value during 2000–2017. Rainfall varied seasonally with 36 consecutive days having no rainfall
310 event (DOY 157–192) and 5 days having successive rainfall events (DOY 237–241) (Fig. 1). The ET_0
(554.7 mm) was approximately twice the rainfall amount during the study period, with the higher and
lower values during the low and high rainfall event periods, respectively (Fig. 1). The SW increased and
subsequently decreased by different degrees following rainfall events, with shallow soil layer (0–30 cm)
exhibited higher variation than the corresponding value below 30 cm in the three plantations (Fig. 1,
315 Table S3). The coefficients of variation (CVs, $SD/mean$) in the shallow soil layer were 18.7%, 16.67%,
and 17.28% in *H. rhamnoides* and *P. tomentosa* pure plantations and the mixed plantation, respectively.
The SW for shallow and middle (30–100 cm) soil layers exhibited lower values than some deep soil
layers (100–200 cm) during the less rainfall event period (such as DOY 157–192) in three plantations.
In addition, compared with shallow and middle soil layers, the deep soil layer SW exhibited a time lag
320 response to rainfall events.

The *H. rhamnoides* and *P. tomentosa* in pure plantations exhibited different fine root vertical

distributions, with more than 40% of fine roots observed in shallow and deep soil layers, respectively (Fig. S4). In the mixed plantation, approximately 40% of *H. rhamnoides* fine roots were in the shallow soil layer. Meanwhile, no significant differences in fine root proportion were observed for *H.*
 325 *rhamnoides* for each soil layer in pure and mixed plantations ($P > 0.05$). The fine root proportion of *P.*
tomentosa in the shallow soil layer was significantly increased from 21.94% in pure plantation to 31.28% in the mixed plantation ($P < 0.05$).

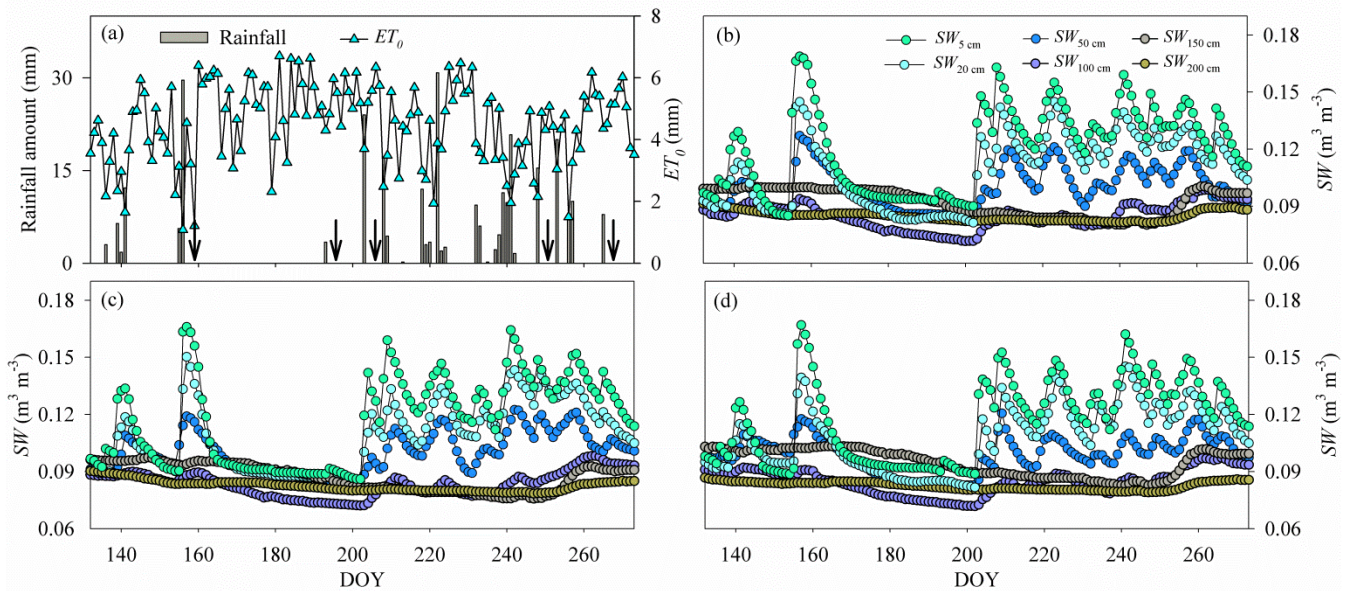


Figure 1. Variation in (a) rainfall amount, reference evapotranspiration (ET_0), and average (mean \pm SD)
 330 soil water content (SW) in (b) *H. rhamnoides* pure plantation, (c) *P. tomentosa* pure plantation, and (d)
 mixed plantation from DOY 132 to 273 (11 May to 30 September) ($n = 3$). Standard deviation bars for
 SW at each soil layers are not shown to allow clear display of variation of SW for each plantation.
 Arrows in (a) indicate dates of sample collection at the first day after rainfall events: DOY 157 (6 June),
 DOY 194 (12 July), DOY 204 (23 July), DOY 249 (6 September), and DOY 265 (22 September).

335

3.2 Variations in sap flow

Daily normalized F_d for *H. rhamnoides* and *P. tomentosa* fluctuated with rainfall events in pure and mixed plantations (Fig. 2). The variation of normalized F_d for *H. rhamnoides* and *P. tomentosa* in mixed plantation was higher than the specific species in pure plantations, with corresponding CVs of 30.99% and 34.88% in the mixed plantation, and 24.64% and 27.44% in pure plantations (Fig. 2). The SF_R after rainfall pulses was significantly influenced by both rainfall amount and plant species ($P < 0.001$) (Fig. 2,
 340

Table S4). Following large rainfall amounts (≥ 15.4 mm), the diurnal variation of sap flow was significantly higher than the value before rainfall ($P < 0.05$) for *H. rhamnoides* in pure plantation and for *P. tomentosa* in both plantation types (Figs. S5 and S6). The lowest rainfall amount (7.9 mm) that significantly increased the diurnal variation of sap flow was observed for *H. rhamnoides* in the mixed plantation (Fig. S5). Furthermore, in response to rainfall pulses, the SF_R for *H. rhamnoides* in pure (range $6.69 \pm 1.22\%$ to $106.34 \pm 4.7\%$) and mixed (range $2.23 \pm 0.54\%$ to $190.89 \pm 15.49\%$) plantations was significantly higher ($P < 0.001$) than corresponding values for *P. tomentosa*: ranges $4.24 \pm 0.52\%$ to $60.28 \pm 5.72\%$ and $3.14 \pm 0.53\%$ to $83.04 \pm 14.23\%$ (Table S4). Mixed afforestation significantly enhanced SF_R for both species ($P < 0.001$) (Table S4).

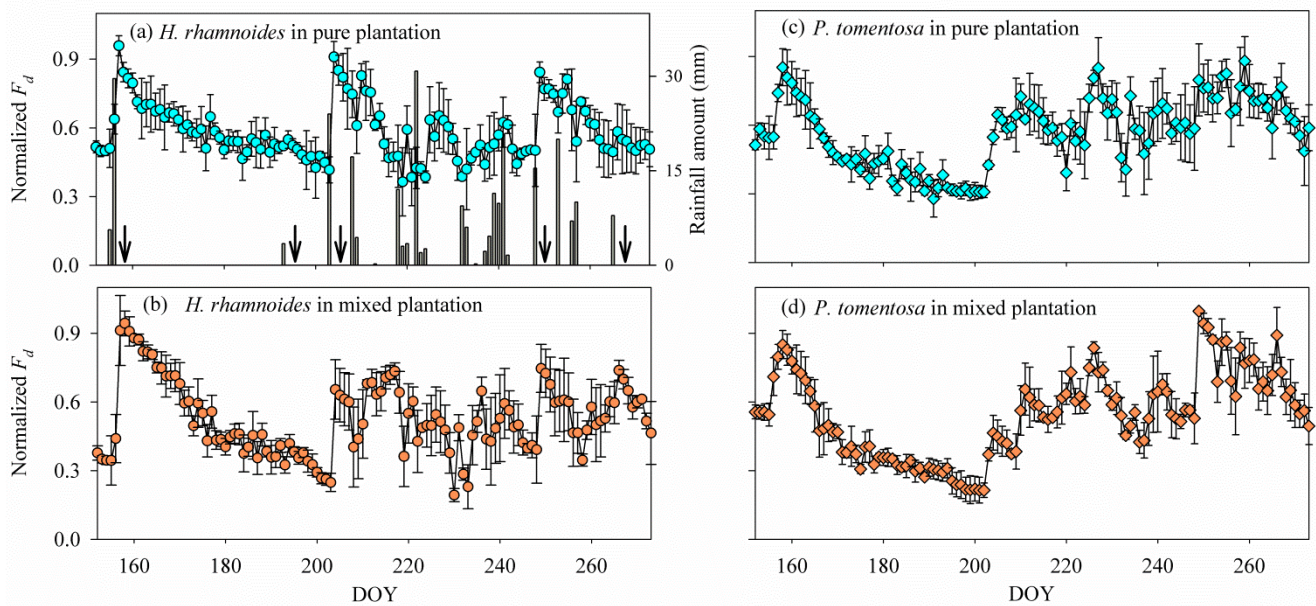


Figure 2. Variation in (a) rainfall amount, and average daily normalized F_d for *H. rhamnoides* in (a) pure and (b) mixed plantations and for *P. tomentosa* in (c) pure and (d) mixed plantations ($n = 3$). Arrows in (a) indicate dates of sample collection at the first day after rainfall events: DOY 157 (6 June), DOY 194 (12 July), DOY 204 (23 July), DOY 249 (6 September), and DOY 265 (22 September).

3.3 Variations in plant water sources

The soil water $\delta^{18}O$ and δD for pure *H. rhamnoides*, pure *P. tomentosa*, and mixed plantations showed large vertical variation following small rainfall events (≤ 7.9 mm), and exhibited relatively small vertical variations following large rainfall events (≥ 15.4 mm) (Fig. S7). The average isotopic values of soil

water depleted from shallow to deep soil layers (Table S3), and water isotopic values in shallow and middle soil layer were close to rainwater in the three plantations following large rainfall events.

Although no significant difference in RUP was observed between *H. rhamnoides* ($14.2 \pm 7.81\%$) and *P. tomentosa* ($12.43 \pm 7.33\%$) in pure plantations (Fig. 3, Table S4), the RUP was significantly higher for *H. rhamnoides* ($19.17 \pm 8.6\%$) than *P. tomentosa* ($14.59 \pm 5.86\%$) in the mixed plantation ($P < 0.05$) (Table S4). In addition, *H. rhamnoides* mainly uptake water from the middle soil layer in pure and mixed plantations based on the MixSIR result, with corresponding average values of $36.27 \pm 2.43\%$ and $44.14 \pm 3.06\%$ (Fig. 4). The water source for *P. tomentosa* in pure and mixed plantations was mainly from the deep and middle soil layers, respectively, with corresponding average values of $41.4 \pm 15.18\%$ and $40.17 \pm 5.9\%$. In pure plantation, the water source from shallow and middle soil layers for *H. rhamnoides* was significantly higher than *P. tomentosa*; however, the water source from the deep soil layer was significantly lower for the former species ($P < 0.05$) (Table S5). No significant differences in water sources from each soil layer were observed between these species in the mixed plantation (Table S5). In addition, mixed afforestation significantly enhanced RUP and decreased the deep soil water uptake proportion for *H. rhamnoides* and *P. tomentosa* ($P < 0.05$) (Table S4, Figs. 3 and 4).

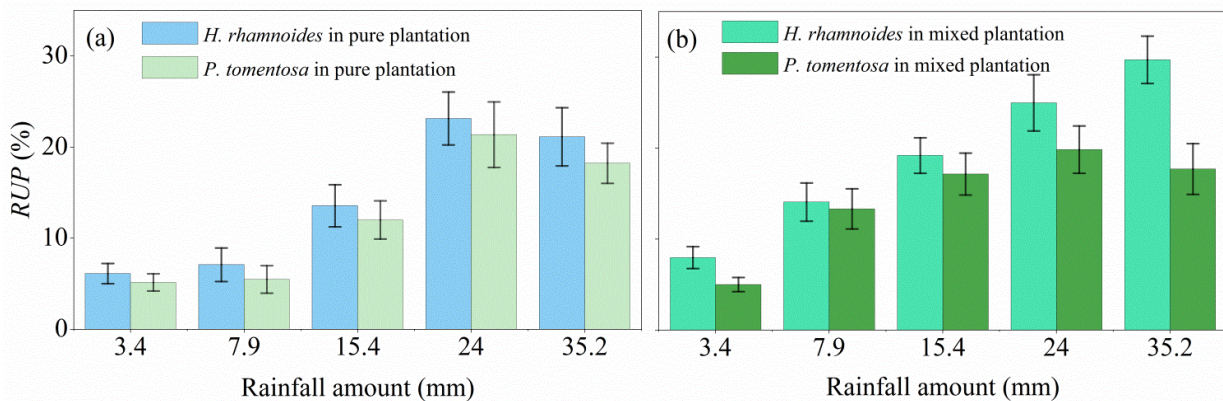


Figure 3. Variation in average rainwater-recharged soil water uptake proportion (RUP) for *H. rhamnoides* and *P. tomentosa* in (a) pure and (b) mixed plantations after five rainfall events ($n = 3$).

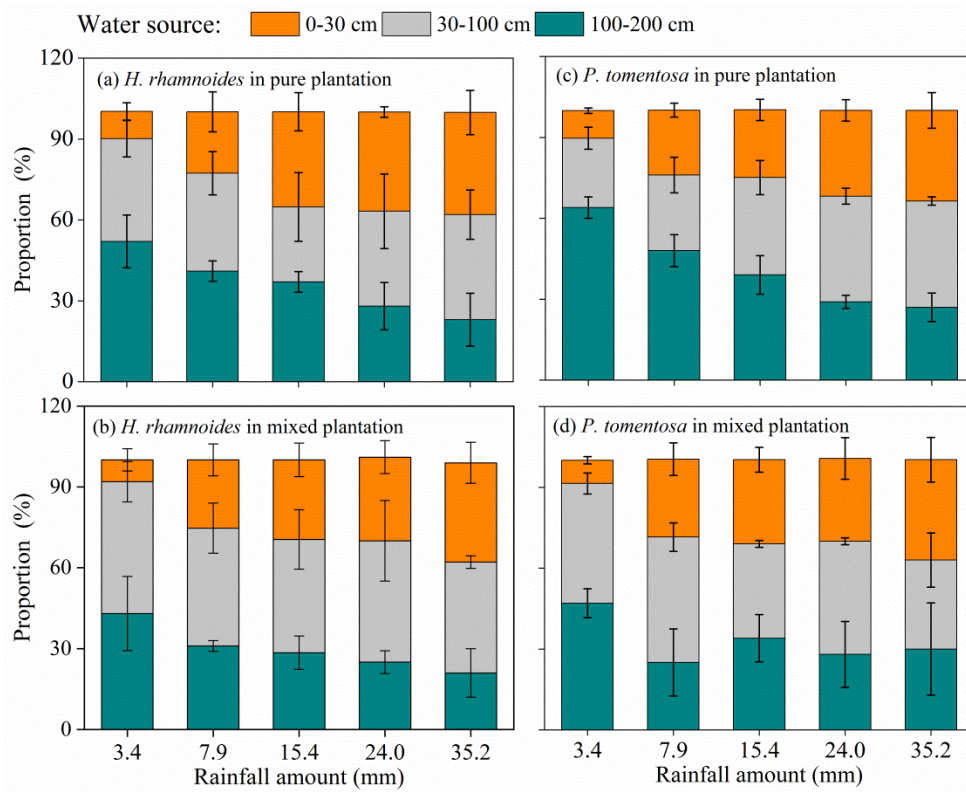
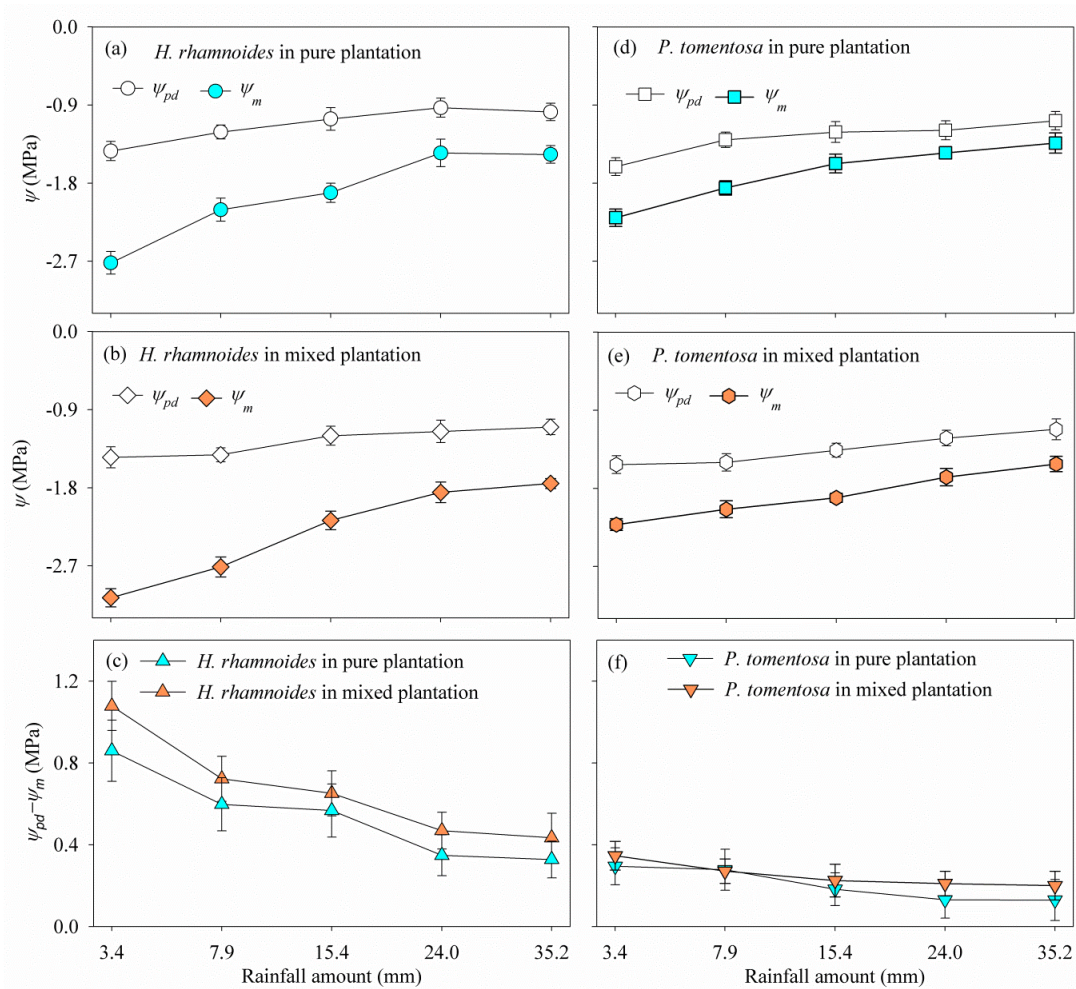


Figure 4. Variation in average plant water sources from three soil layers (0–30, 30–100, and 100–200 cm) for *H. rhamnoides* in (a) pure and (b) mixed plantations, and for *P. tomentosa* in (c) pure and (d) mixed plantations after five rainfall events ($n = 3$).

3.4 Variations in plant leaf water potential

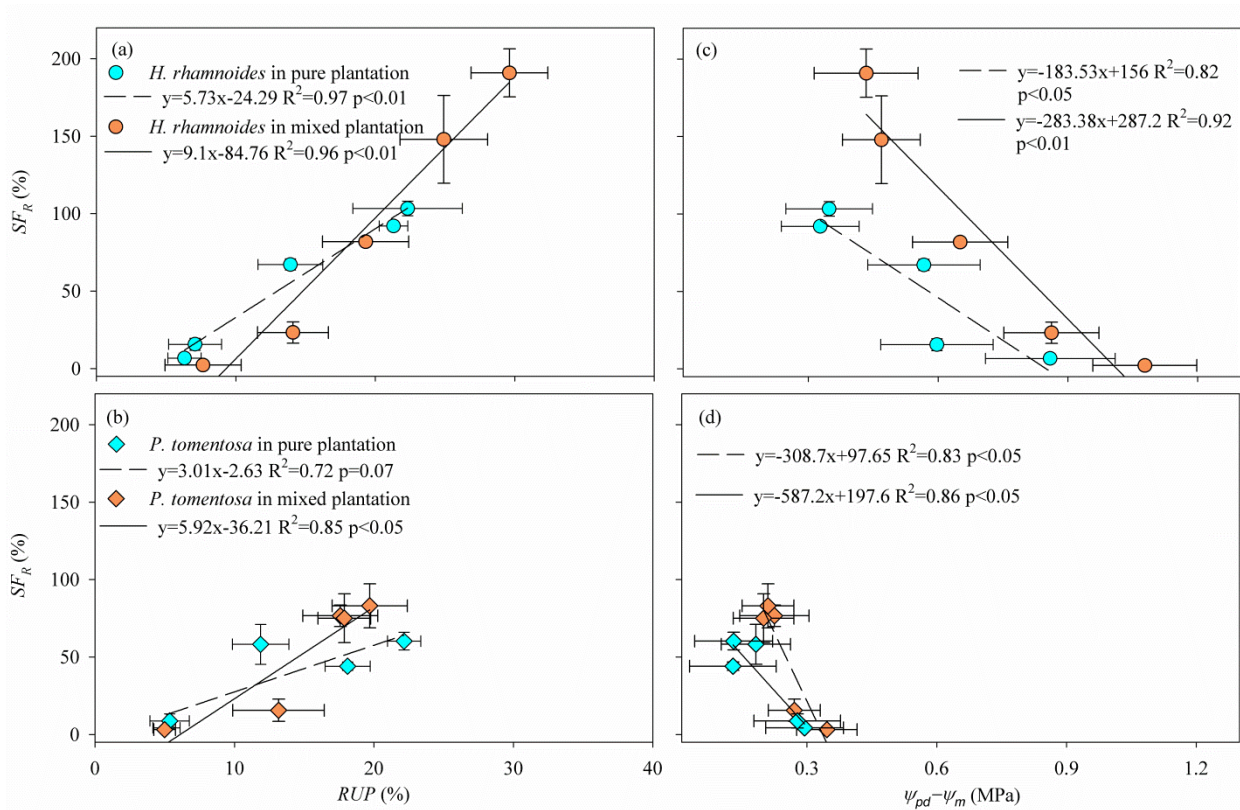
In response to rainfall pulses, *H. rhamnoides* exhibited higher CVs for Ψ_{pd} , Ψ_m , and $\Psi_{pd}-\Psi_m$ than corresponding values for *P. tomentosa* in both plantation types, except that *H. rhamnoides* exhibited lower CVs for Ψ_{pd} than *P. tomentosa* (12.99% and 18.33%, respectively) in the mixed plantation (Fig. 5). Compared with *P. tomentosa*, *H. rhamnoides* exhibited significantly positive Ψ_{pd} in the pure plantation, negative Ψ_m in the mixed plantation, and larger $\Psi_{pd}-\Psi_m$ in both plantation types ($P < 0.05$) (Table S6). Meanwhile, mixed afforestation significantly reduced the Ψ_m and increased the Ψ_{pd} for *H. rhamnoides* and *P. tomentosa* ($P < 0.05$), respectively, and significantly increased $\Psi_{pd}-\Psi_m$ for both species (Table S6).



395 **Figure 5.** Variation in average plant predawn (Ψ_{pd}), midday leaf water potential (Ψ_m), and leaf water potential gradient ($\Psi_{pd} - \Psi_m$) for (a–c) *H. rhamnoides* and (d–f) *P. tomentosa* in both plantation types after five rainfall events ($n = 3$).

3.5 Influence of water sources and $\Psi_{pd} - \Psi_m$ on plant transpiration

400 The SF_R significantly increased with increasing RUP and decreasing $\Psi_{pd} - \Psi_m$ for *H. rhamnoides* ($P < 0.01$) in both plantation types (Fig. 6). Meanwhile, SF_R significantly increased with decreasing $\Psi_{pd} - \Psi_m$ for *P. tomentosa* in both plantation types ($P < 0.05$). However, a significant relationship between SF_R and RUP was observed for *P. tomentosa* in the mixed ($P < 0.05$) but not in pure plantations (Fig. 6).



405 **Figure 6.** Relationship of average (a, b) rainwater-recharged soil water uptake proportion (RUP) and (c, d) leaf water potential gradient ($\Psi_{pd} - \Psi_m$) with relative response of normalized F_d (SF_R) for *H. rhamnoides* and *P. tomentosa* in both plantation types ($n = 3$).

4 Discussion

410 4.1 RRS uptake enhances plant transpiration for *H. rhamnoides* but not *P. tomentosa* in pure plantations

Rainwater is the only replenished soil water source in the studied region (Shao et al., 2018), because plants cannot uptake ground water of approximately 150 m depth below the surface, which was determined through well observation (unpublished data). Small rainfall events generally only wet the soil surface and may evaporate before plant root uptake (Gebauer and Ehleringer, 2000). However, large rainfall events are most likely recharge soil water and enhance the metabolic activity of plant fine roots (Hudson et al., 2018), thus enhancing plant water uptake. Furthermore, the $\delta^{18}O$ and δD values in small rainfall events generally exhibit more positive values than those in large rainfall events (Fig. S7).

Salamalikis et al. (2016) attribute this phenomenon to the sub-cloud evaporation effect in dry conditions where rainwater in small rainfall event is more vulnerable subject to evaporation during their descent

process compared in large rainfall event. Similar to *Salix psammophila* and *Caragana korshinskii* in the studied region (Zhao et al., 2021), both *H. rhamnoides* and *P. tomentosa* exhibited plasticity in water sources in pure plantations (Fig. 4), with *H. rhamnoides* exhibiting the greater plasticity. In pure plantations, the obviously lower SWC at all soil depths (Fig. 1) and large water uptake proportion from the deep soil layer (Fig. 4) after 3.4 mm of rainfall for these two species, suggested that this rainfall amount did not relieve the drought caused by 36 days (DOY 157–192) of no rainfall. The RUP for *H. rhamnoides* but not *P. tomentosa* significantly increased following an increase in rainfall amount ($P < 0.05$) (Fig. S8), indicating that water uptake was more sensitive to rainfall pulse for *H. rhamnoides*. This may be mainly due to the greater proportions of fine root surface area distributed in the shallow soil layer for *H. rhamnoides* ($40.85 \pm 3.14\%$) compared to *P. tomentosa* ($21.94 \pm 2.3\%$) (Fig. S4).

The RRS uptake does not permit plant transpiration increase after rainfall pulses especially in semiarid and arid environments (Grossiord et al., 2017; West et al., 2007), and the influence of water potential gradient ($\Psi_{pd} - \Psi_m$) on plant transpiration should also be considered (Hudson et al., 2018; Kumagai and Porporato, 2012). For example, although *Juniperus osteosperma*, a deep rooted plant species, could uptake RRS after large rainfall events in the west of the United States, the plant transpiration did not increase with increasing rainfall amount (West et al., 2007). The asynchronization between RRS uptake and plant transpiration for *J. osteosperma* was mainly attributed to the uptake of RRS by plants being unable to reverse the cavitation in its roots and stems (Grossiord et al., 2017; West et al., 2007). Our previous investigations in the studied region indicated that *P. tomentosa* is relatively more vulnerable to cavitation than *H. rhamnoides*, with water potential at 50% loss of conductivity of -1.15 MPa (Zhang et al., 2013) and -1.49 MPa (Dang et al., 2017), respectively, based on stem vulnerability curves. Being less vulnerable to stem cavitation allowed *H. rhamnoides* to experience a significantly lower Ψ_m and larger $\Psi_{pd} - \Psi_m$ compared with *P. tomentosa* in response to soil water conditions after rainfall pulses. The large $\Psi_{pd} - \Psi_m$ for *H. rhamnoides* was consistent with the high SF_R and CVs of normalized sap flow, indicating that this species exhibited a rainfall sensitive mechanism. The relative constant $\Psi_{pd} - \Psi_m$ for *P. tomentosa* was consistent with the relatively small SF_R and CVs of normalized sap flow, indicating that this species exhibited a rainfall insensitive mechanism.

Furthermore, after rainfall events, the SF_R for *H. rhamnoides* but not for *P. tomentosa* significantly increased following rainfall amount increases ($P < 0.05$) (Fig. S8), also indicating that plant
450 transpiration was more sensitive to rainfall pulses for *H. rhamnoides*.

Consistent with the first hypothesis, the influence of RRS uptake and $\Psi_{pd}-\Psi_m$ on SF_R was different for these species in pure plantations. The SF_R was significantly influenced by RUP and $\Psi_{pd}-\Psi_m$ for *H. rhamnoides* in the pure plantation, indicating that RRS uptake and leaf physiological adjustment enhanced its plant transpiration (Figs. 6 and 7). However, the SF_R was significantly influenced by
455 $\Psi_{pd}-\Psi_m$ for *P. tomentosa* (Fig. 6), suggesting that its transpiration was mainly constrained by plant physiological characteristics. The ET_0 represents the atmospheric evaporative demand, and has been observed to influence plant transpiration in water limited (Li et al., 2021) and non-water limited regions (Iida et al., 2016). However, in the present study, neither ET_0 after rainfall nor relative response of ET_0 significantly influenced SF_R for either species in pure plantations (Table S7). The influence of plant
460 physiological characteristics (i.e. $\Psi_{pd}-\Psi_m$) on SF_R for both species, may partially contribute to the lack of atmosphere evaporative demand effect on plant transpiration in the studied region, although these species exhibited different rainfall pulse sensitivity.

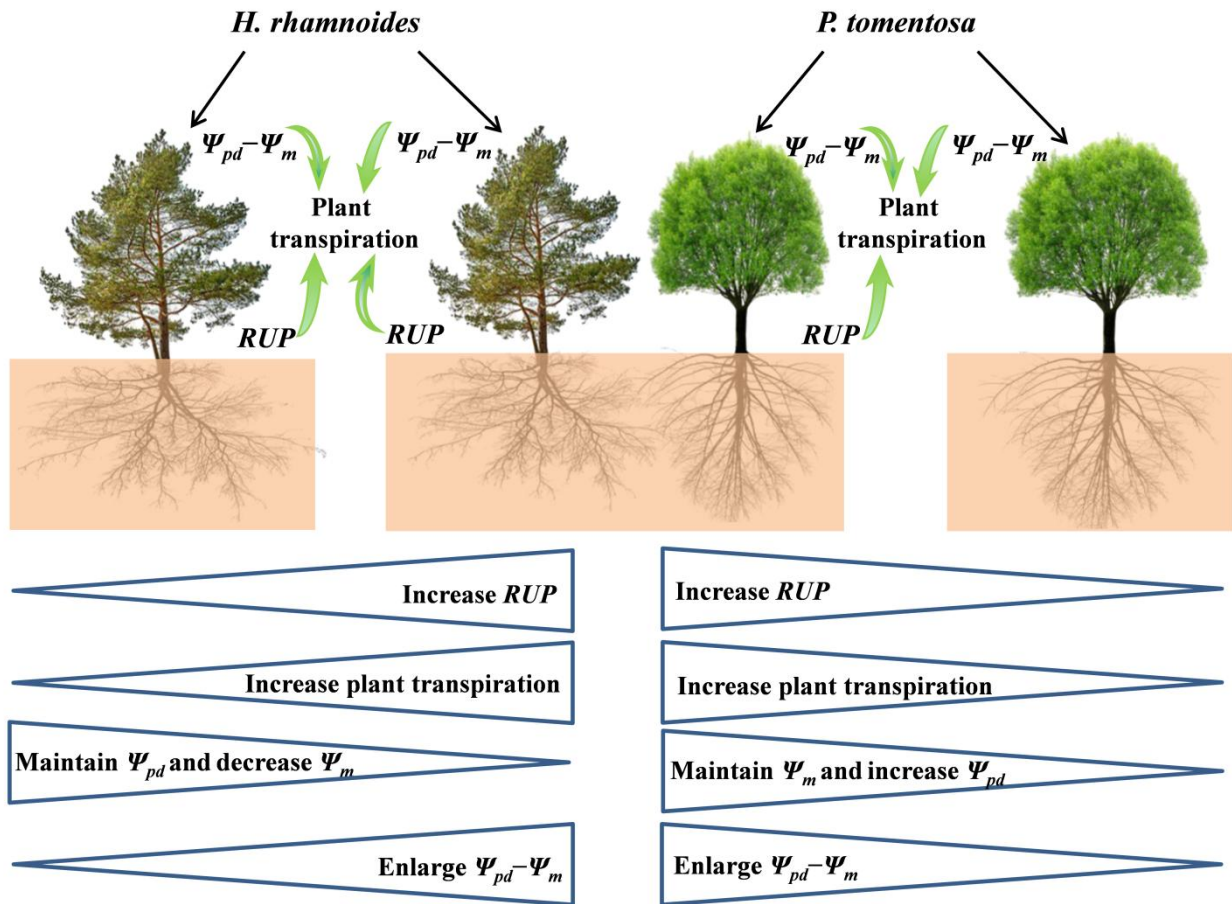


Figure 7. Schematic of rainwater-recharged soil water (RRS) uptake, leaf water potential gradient, and plant transpiration for *H. rhamnoides* and *P. tomentosa* in both plantation types. Both RRS uptake proportion (RUP) and leaf water potential gradient ($\Psi_{pd}-\Psi_m$) enhanced plant transpiration after rainfall pulses for *H. rhamnoides* in pure and mixed plantations, and for *P. tomentosa* in mixed plantation. However, $\Psi_{pd}-\Psi_m$ rather than RUP significantly influenced plant transpiration after rainfall pulses for *P. tomentosa* in the pure plantation. Mixed afforestation effect of these parameters for each species are indicated at the bottom half of the schematic, with “increase”, “decrease” or “enlarge” indicating a significant difference ($P < 0.05$) for a species between pure and mixed plantations. Mixed afforestation significantly enhanced RUP and plant transpiration, decreased Ψ_m , and enlarged $\Psi_{pd}-\Psi_m$ for *H. rhamnoides*, and also significantly enhanced the RUP and plant transpiration, increased Ψ_{pd} , and enlarged $\Psi_{pd}-\Psi_m$ for *P. tomentosa*.

4.2 RRS uptake enhances plant transpiration for coexisting species in mixed plantation

Spatial water resource partitioning is considered one of the essential plant strategies to maintain coexistence in mixed plantations, especially in semiarid and arid regions (Munoz-Villers et al., 2020; Silvertown et al., 2015; Yang et al., 2020). However, water source competition has widely been
480 observed among coexisting plant species according to the literature surveys by Silvertown et al. (2015) and Tang et al. (2018), in either water sufficient or limited regions. In the present study, the non-significant differences in xylem $\delta^{18}\text{O}$ and δD ($P > 0.05$) and plant water sources for the three soil layers (Fig. 4, Table S5) indicated water competition between these species in the mixed plantation, although the RUP was significantly higher for *H. rhamnoides* (Table S4).

485 Generally, two types of adaptation can be adopted by plants to cope with resource competition: increased competition ability or minimized competition interactions (West et al., 2007). Consistent with the first adaptation type, mixed afforestation enhanced the RUP for *H. rhamnoides* and *P. tomentosa* (Figs. 3 and 7, Table S4). Although mixed afforestation did not significantly alter the Ψ_{pd} and Ψ_{m} for *H. rhamnoides* and *P. tomentosa*, respectively, significantly negative Ψ_{m} and positive Ψ_{pd} were observed
490 for corresponding species ($P < 0.01$) (Table S6). Mixed afforestation significantly increased Ψ_{pd} for *P. tomentosa*, possibly due to the advantage of access to soil moisture recharged by rainwater through an increased root surface area in the shallow soil layer for this species in the mixed plantation (Fig. S4). Thus, plant physiological (Ψ_{m}) and root morphological adjustments were adopted by *H. rhamnoides* and *P. tomentosa* in the mixed plantation, respectively, to significantly enlarge $\Psi_{\text{pd}} - \Psi_{\text{m}}$ and increase RUP
495 (Fig. 7). The different influence of RUP and $\Psi_{\text{pd}} - \Psi_{\text{m}}$ on SF_{R} for specific species in pure and mixed plantations was consistent with the second hypothesis. The significant influence of RUP and $\Psi_{\text{pd}} - \Psi_{\text{m}}$ on SF_{R} was observed for *P. tomentosa* in mixed plantation (Fig. 6). Meanwhile, for *H. rhamnoides* in mixed plantation compared to specific value in pure plantation, larger and smaller slopes in linear regression were observed between SF_{R} and RUP, and SF_{R} and $\Psi_{\text{pd}} - \Psi_{\text{m}}$, respectively (Fig. 6). Similar to
500 the result in pure plantations, no significant relationship between SF_{R} and ET_0 after rainfall and relative response of ET_0 was observed for these species in the mixed plantation (Table S7). This result also confirmed the influence of physiological or morphological factors on plant transpiration for these species in the mixed plantation in response to rainfall pulses.

Furthermore, similar to other studies in the Loess Plateau (Wang et al., 2020a; Wu et al., 2021), the
505 deep soil layer generally exhibited lower SW than other soil layers in all plantation types in the present
study (Fig. 1, Table S3). Jia et al. (2017) and Wang et al. (2020a) attributed the lower SW in deep soil
layers to the imbalance between rainwater replenishment and plant uptake of water from this soil layer
in the studied region. Silvertown et al. (2015) and Tang et al. (2019) suggested that coexisting plant
species generally reduce water uptake from soil layers that exhibit low soil water content to avoid water
510 source competition in these layers and maintain stable coexistence. In the present study, consistent with
the second adaptation type, mixed afforestation significantly decreased the water uptake proportion
from the deep soil layer for these species (Table S5). Thus, both increased rainwater-recharged soil
water uptake and decreased water source competition from the deep soil layer were adopted by these
species in the mixed plantation to minimize water sources competition under water limited conditions.

515

4.3 Implications for plantation species and type selection based on RRS uptake and plant transpiration

The RRS uptake and plant transpiration in response to rainfall pulses may influence plant
physiological process and the water cycle (Meier et al., 2018; Zhao et al., 2021). In pure plantations, *H.*
520 *rhamnoides* rather than *P. tomentosa* showed an advantage in RRS uptake due to the large $\Psi_{pd}-\Psi_m$ and
high fine root surface area proportions distributed in the shallow soil layer for the former species,
although both species exhibited plasticity in water sources. The excessive water uptake from the deep
soil may desiccate deep soil (Wu et al., 2021), weakening plant resilience to drought stress and thus
plant community sustainability in this Loess Plateau region (Song et al., 2018; Zhao et al., 2021). West
525 et al. (2012) and Wu et al. (2021) suggested that increased RRS uptake can reduce plant water uptake
from deep soil layers, and is essential for plantation adaptation in water limited regions. In the present
study, physiological (e.g., Ψ_m) and morphological (fine root distribution) adjustments were observed for
H. rhamnoides and *P. tomentosa* in the mixed plantation, respectively, to enlarge $\Psi_{pd}-\Psi_m$ and enhance
the RUP and plant transpiration (Figs. 7 and S4). The significantly increased RUP and decreased deep
530 soil water uptake proportion for both species in mixed plantation may relieve deep soil water deficit and

strengthen plantation sustainability (Tables S4 and S5). Furthermore, mixed afforestation also increased the total biomass of *H. rhamnoides* and *P. tomentosa*, calculated through the allometric equation indicated in Zhou et al. (2018) and Tang et al. (2019) (Table S8). Thus, rainfall pulse sensitive species in pure plantation, and plant species in mixed plantation that can adopt physiological or morphological adjustment to enhance rainwater-recharged soil water uptake and reduce excessive water uptake from deep soil layers, should be more often considered for use in the studied region.

5 Conclusions

The influence of water sources and $\Psi_{pd}-\Psi_m$ on plant transpiration in response to rainfall pulses was determined for *H. rhamnoides* and *P. tomentosa* in the semiarid Loess Plateau region. In pure plantations, the SF_R was significantly influenced by RUP and $\Psi_{pd}-\Psi_m$ for *H. rhamnoides*, but the SF_R was significantly influenced by $\Psi_{pd}-\Psi_m$ for *P. tomentosa*. Meanwhile, the lower value $\Psi_{pd}-\Psi_m$ was consistent with the high SF_R for *H. rhamnoides*, and the higher value $\Psi_{pd}-\Psi_m$ was consistent with the low SF_R for *P. tomentosa*, in response to rainfall pulses. Thus, *H. rhamnoides* and *P. tomentosa* exhibited sensitive and insensitive response to rainfall pulses, respectively. Furthermore, mixed afforestation enhanced the RRS uptake and plant transpiration for both species. Significantly lower plant Ψ_m and increased fine root surface area were adopted by *H. rhamnoides* and *P. tomentosa* in the mixed plantation, respectively, to enlarge $\Psi_{pd}-\Psi_m$ and enhance RRS uptake and decrease water source competition from the deep soil layer. The SF_R was significantly influenced by RUP and $\Psi_{pd}-\Psi_m$ for both species in the mixed plantation, and RRS uptake enhanced plant transpiration in the mixed plantation regardless of species sensitivity to rainfall pulses.

Data availability

The data that support the findings of this study are available from the corresponding author upon request.

Author contribution

YKT designed the study, performed the statistical analyses and wrote the original manuscript draft.

LNW and YQY performed the experiments and collected the data. DXL collected the data.

560

Declaration of Competing Interest

The authors declare that they have no conflict of interest.

Acknowledgement

565 This work was supported by the National Natural Science Foundation of China (41977425), the National Key Research and Development Program of China (2017YFA0604801). We acknowledge the insightful suggestions of editor and reviewers.

References

- 570 Allen, R.G., Periera, L.S., Raes, D., and Smith, M.: Crop evapotranspiration: Guidelines for Computing Crop Requirements, Irrigation and Drainage paper NO.56, FAO, Rome, Italy, 300, 1998.
- Bai, X., Jia, X. X., Jia, Y. H., Shao, M. A., and Hu, W.: Modeling long-term soil water dynamics in response to land-use change in a semi-arid area, *J Hydrol*, 585, 2020.
- Berkelhammer, M., Still, C., Ritter, F., Winnick, M., Anderson, L., Carroll, R., Carbone, M., and
575 Williams, K. H.: Persistence and Plasticity in Conifer Water-Use Strategies, *J Geophys Res-Bioge*, 125, 10.1029/2018JG004845, 2020.
- Chen, Y. J., Cao, K. F., Schnitzer, S. A., Fan, Z. X., Zhang, J. L., and Bongers, F.: Water-use advantage for lianas over trees in tropical seasonal forests, *New Phytol*, 205, 128-136, 2015.
- Cheng, X. L., An, S. Q., Li, B., Chen, J. Q., Lin, G. H., Liu, Y. H., Luo, Y. Q., and Liu, S. R.: Summer
580 rain pulse size and rainwater uptake by three dominant desert plants in a desertified grassland ecosystem in northwestern China, *Plant Ecol*, 184, 1-12, 2006.
- Dang, E., Jiang, Z.M., Li, R., Zhang, S.X., and Cai, J.: Relationship between hydraulic traits and refilling of embolism in the xylem of one-year-old twigs of six tree species, *Scientia Silvae Sinicae*, 53, 49-59, 10.11707/j.1001-7488, 2017. (In Chinese with English abstract)

- 585 Du, S., Wang, Y. L., Kume, T., Zhang, J. G., Otsuki, K., Yamanaka, N., and Liu, G. B.: Sapflow characteristics and climatic responses in three forest species in the semiarid Loess Plateau region of China, *Agr Forest Meteorol*, 151, 1-10, 2011.
- Ellsworth, P. Z., and Williams, D. G.: Hydrogen isotope fractionation during water uptake by woody xerophytes, *Plant Soil*, 291, 93-107, 10.1007/s11104-006-9177-1, 2007.
- 590 Gebauer, R. L. E., and Ehleringer, J. R.: Water and nitrogen uptake patterns following moisture pulses in a cold desert community, *Ecology*, 81, 1415-1424, 2000.
- Granier, A.: Evaluation of transpiration in a Douglas-fir stand by means of sap flow measurements, *Tree Physiology*, 3, 309-320, 1987.
- Grossiord, C., Sevanto, S., Dawson, T. E., Adams, H. D., Collins, A. D., Dickman, L. T., Newman, B.
- 595 D., Stockton, E. A., and McDowell, N. G.: Warming combined with more extreme precipitation regimes modifies the water sources used by trees, *New Phytol*, 213, 584-596, 10.1111/nph.14192, 2017.
- Hudson, P. J., Limousin, J. M., Krofcheck, D. J., Boutz, A. L., Pangle, R. E., Gehres, N., McDowell, N. G., and Pockman, W. T.: Impacts of long-term precipitation manipulation on hydraulic architecture and xylem anatomy of pinon and juniper in Southwest USA, *Plant Cell Environ*, 41, 421-435,
- 600 10.1111/pce.13109, 2018.
- Iida, S., Shimizu, T., Tamai, K., Kabeya, N., Shimizu, A., Ito, E., Ohnuki, Y., Chann, S., and Keth, N.: Interrelationships among dry season leaf fall, leaf flush and transpiration: insights from sap flux measurements in a tropical dry deciduous forest, *Ecohydrology*, 9, 472-486, 10.1002/eco.1650, 2016.
- Jia, X. X., Zhao, C. L., Wang, Y. Q., Zhu, Y. J., Wei, X. R., and Shao, M. A.: Traditional dry soil layer
- 605 index method overestimates soil desiccation severity following conversion of cropland into forest and grassland on China's Loess Plateau, *Agr Ecosyst Environ*, 291, Artn 106794, 10.1016/J.Agee.2019.106794, 2020.
- Kumagai, T., and Porporato, A.: Strategies of a Bornean tropical rainforest water use as a function of rainfall regime: isohydric or anisohydric?, *Plant Cell Environ*, 35, 61-71,
- 610 10.1111/j.1365-3040.2011.02428.x, 2012.
- Li, H. Q., Zhang, F. W., Zhu, J. B., Guo, X. W., Li, Y. K., Lin, L., Zhang, L. M., Yang, Y. S., Li, Y. N.,

- Cao, G. M., Zhou, H. K., and Du, M. Y.: Precipitation rather than evapotranspiration determines the warm-season water supply in an alpine shrub and an alpine meadow, *Agr Forest Meteorol*, 300, ARTN 108318, 10.1016/j.agrformet.2021.108318, 2021.
- 615 Liu, G. B., Shangguan, Z. P., Yao, W. Y., Yang, Q. K., Zhao, M. J., Dang, X. H., Guo, M. H., Wang, G. L., and Wang, B.: Ecological effects of soil conservation in Loess Plateau, *Bull Chin Acad Sci*, 32, 11–19, 10.16418/j.issn.1000-3045.2017.01.002, 2017. (In Chinese with English abstract)
- Liu, Z. Q., Yu, X. X., and Jia, G. D.: Water uptake by coniferous and broad-leaved forest in a rocky mountainous area of northern China, *Agr Forest Meteorol*, 265, 381-389, 620 10.1016/j.agrformet.2018.11.036, 2019.
- Meier, I. C., Knutzen, F., Eder, L. M., Muller-Haubold, H., Goebel, M. O., Bachmann, J., Hertel, D., and Leuschner, C.: The Deep Root System of *Fagus sylvatica* on Sandy Soil: Structure and Variation Across a Precipitation Gradient, *Ecosystems*, 21, 280-296, 10.1007/s10021-017-0148-6, 2018.
- Mendham, D. S., White, D. A., Battaglia, M., McGrath, J. F., Short, T. M., Ogden, G. N., and Kinal, J.: 625 Soil water depletion and replenishment during first- and early second-rotation *Eucalyptus globulus* plantations with deep soil profiles, *Agr Forest Meteorol*, 151, 1568-1579, 10.1016/j.agrformet.2011.06.014, 2011.
- Moore, J. W., and Semmens, B. X.: Incorporating uncertainty and prior information into stable isotope mixing models, *Ecol Lett*, 11, 470-480, 10.1111/j.1461-0248.2008.01163.x, 2008.
- 630 Munoz-Villers, L. E., Geris, J., Alvarado-Barrientos, M. S., Holwerda, F., and Dawson, T.: Coffee and shade trees show complementary use of soil water in a traditional agroforestry ecosystem, *Hydrol Earth Syst Sc*, 24, 1649-1668, 10.5194/hess-24-1649-2020, 2020.
- Plaut, J. A., Wadsworth, W. D., Pangle, R., Yepez, E. A., McDowell, N. G., and Pockman, W. T.: 635 Reduced transpiration response to precipitation pulses precedes mortality in a pinon-juniper woodland subject to prolonged drought, *New Phytol*, 200, 375-387, 10.1111/nph.12392, 2013.
- Reynolds, W.D., Elrick, D.E., Youngs, E.G., Booltink, H.W.G., and Bouma, J.: Saturated and field-saturated water flow parameters, in: *Methods of soil analysis*, edited by: Dane, J.H., Topp, G.C., Soil Science Society of America, Madison, Wisconsin, USA, 797-878, 2002.

- Salamalikis, V., Argiriou, A. A., and Dotsika, E.: Isotopic modeling of the sub-cloud evaporation effect
640 in precipitation, *Sci Total Environ*, 544, 1059-1072, 2016.
- Shao, J., Si, B. C., and Jin, J. M.: Extreme Precipitation Years and Their Occurrence Frequency
Regulate Long-Term Groundwater Recharge and Transit Time, *Vadose Zone J*, 17, 2018.
- Silvertown, J., Araya, Y., and Gowing, D.: Hydrological niches in terrestrial plant communities: a
review, *J Ecol*, 103, 93-108, 10.1111/1365-2745.12332, 2015.
- 645 Šimůnek, J., van Genuchten, M. T., and Šejna, M.: Development and applications of the HYDRUS and
STANMOD software packages and related codes, *Vadose Zone J*, 7, 587-600, 2008.
- Song, X. P., Hansen, M. C., Stehman, S. V., Potapov, P. V., Tyukavina, A., Vermote, E. F., and
Townshend, J. R.: Global land change from 1982 to 2016, *Nature*, 560, 639,
10.1038/s41586-018-0411-9, 2018.
- 650 Stahl, C., Herault, B., Rossi, V., Burban, B., Brechet, C., and Bonal, D.: Depth of soil water uptake by
tropical rainforest trees during dry periods: does tree dimension matter ?, *Oecologia*, 173, 1191-1201,
10.1007/s00442-013-2724-6, 2013.
- Steppe, K., De Pauw, D. J. W., Doody, T. M., and Teskey, R. O.: A comparison of sap flux density
using thermal dissipation, heat pulse velocity and heat field deformation methods, *Agr Forest Meteorol*,
655 150, 1046-1056, 10.1016/j.agrformet.2010.04.004, 2010.
- Swaffer, B. A., Holland, K. L., Doody, T. M., Li, C., and Hutson, J.: Water use strategies of two
co-occurring tree species in a semi-arid karst environment, *Hydrol Process*, 28, 2003-2017,
10.1002/hyp.9739, 2014.
- Tang, Y. K., Wu, X., Chen, Y. M., Wen, J., Xie, Y. L., and Lu, S. B.: Water use strategies for two
660 dominant tree species in pure and mixed plantations of the semiarid Chinese Loess Plateau,
Ecohydrology, 11, Artn E1943, 10.1002/Eco.1943, 2018.
- Tang, Y. K., Wu, X., Chen, C., Jia, C., and Chen, Y. M.: Water source partitioning and nitrogen
facilitation promote coexistence of nitrogen-fixing and neighbor species in mixed plantations in the
semiarid Loess Plateau, *Plant Soil*, 445, 289-305, 10.1007/s11104-019-04301-9, 2019.
- 665 Tfwala, C. M., van Rensburg, L. D., Bello, Z. A., and Zietsman, P. C.: Transpiration dynamics and

- water sources for selected indigenous trees under varying soil water content, *Agr Forest Meteorol*, 275, 296-304, 10.1016/j.agrformet.2019.05.030, 2019.
- Wang, J., Fu, B. J., Wang, L. X., Lu, N., and Li, J. Y.: Water use characteristics of the common tree species in different plantation types in the Loess Plateau of China, *Agr Forest Meteorol*, 288, ARTN 108020, 10.1016/j.agrformet.2020.108020, 2020a.
- 670
- Wang, S. F., An, J., Zhao, X. N., Gao, X. D., Wu, P., Huo, G. P., and Robinson, B. H.: Age- and climate- related water use patterns of apple trees on China's Loess Plateau, *J Hydrol*, 582, 2020b.
- West, A. G., Hultine, K. R., Jackson, T. L., and Ehleringer, J. R.: Differential summer water use by *Pinus edulis* and *Juniperus osteosperma* reflects contrasting hydraulic characteristics, *Tree Physiol*, 27, 1711-1720, 10.1093/treephys/27.12.1711, 2007.
- 675
- West, A. G., Dawson, T. E., February, E. C., Midgley, G. F., Bond, W. J., and Aston, T. L.: Diverse functional responses to drought in a Mediterranean-type shrubland in South Africa, *New Phytol*, 195, 396-407, 10.1111/j.1469-8137.2012.04170.x, 2012.
- Wu, G. L., Yang, Z., Cui, Z., Liu, Y., Fang, N. F., and Shi, Z. H.: Mixed artificial grasslands with more roots improved mine soil infiltration capacity, *J Hydrol*, 535, 54-60, 2016.
- 680
- Wu, W. J., Li, H. J., Feng, H., Si, B. C., Chen, G. J., Meng, T. F., Li, Y., and Siddique, K. H. M.: Precipitation dominates the transpiration of both the economic forest (*Malus pumila*) and ecological forest (*Robinia pseudoacacia*) on the Loess Plateau after about 15 years of water depletion in deep soil, *Agr Forest Meteorol*, 297, ARTN 108244, 10.1016/j.agrformet.2020.108244, 2021.
- 685
- Xi, B. Y., Wang, Y., Jia, L. M., Bloomberg, M., Li, G. D., and Di, N.: Characteristics of fine root system and water uptake in a triploid *Populus tomentosa* plantation in the North China Plain: Implications for irrigation water management, *Agr Water Manage*, 117, 83-92, 2013.
- Yang, B., Wen, X. F., and Sun, X. M.: Seasonal variations in depth of water uptake for a subtropical coniferous plantation subjected to drought in an East Asian monsoon region, *Agr Forest Meteorol*, 201, 218-228, 10.1016/j.agrformet.2014.11.020, 2015.
- 690
- Yang, B., Meng, X. J., Singh, A. K., Wang, P. Y., Song, L., Zakari, S., and Liu, W. J.: Intercrops improve surface water availability in rubber-based agroforestry systems, *Agr Ecosyst Environ*, 298,

Artn 106937, 10.1016/J.Agee.2020.106937, 2020.

695 Yi, C. Q., and Fan, J.: Application of HYDRUS-1D model to provide antecedent soil water contents for analysis of runoff and soil erosion from a slope on the Loess Plateau, *Catena*, 139, 1-8, 2016.

Zhang, H. D., Wei, W., Chen, L. D., and Yang, L.: Evaluating canopy transpiration and water use of two typical planted tree species in the dryland Loess Plateau of China, *Ecohydrology*, 10, Artn E1830, 10.1002/Eco.1830, 2017.

700 Zhang, H.X., L, S., Zhang, S.X., Xiong, X.Y., and Cai, J.: Relationships between xylem vessel structure and embolism vulnerability in four *Populus* clones, *Scientia Silvae Sinicae*, 49, 54-61, 10.11707 / j.1001-7488.20130508, 2013. (In Chinese with English abstract)

Zhao, Y., Wang, L., Knighton, J., Evaristo, J., and Wassen, M.: Contrasting adaptive strategies by *Caragana korshinskii* and *Salix psammophila* in a semiarid revegetated ecosystem, *Agr Forest Meteorol*, 300, ARTN 108323, 10.1016/j.agrformet.2021.108323, 2021.

705 Zhou, G.Y., Yin, G.C., Tang, X.L., Wen, Z.D., Liu, C.P., Kuang, Y.W., and Wang, W.T.: Carbon reserves in forest ecosystems of China: Biomass allometric equation. Science Press, Beijing, China, 44-54, 2018. (In Chinese).